

SUPPORTING INFORMATION

Journal: **ENVIRONMENTAL SCIENCE & TECHNOLOGY**

MS No.: es-2011-034087

Pages: 11

Figures: 4

Tables: 1

Equations: 12

Exploring How Organic Matter Controls Structural Transformations In Natural Aquatic Nanocolloidal Dispersions

Stephen M. King^{1,} and Helen P. Jarvie²*

¹ ISIS Facility, STFC Rutherford Appleton Laboratory, Harwell Oxford, Didcot OX11 0QX, UK

² Centre for Ecology & Hydrology, Maclean Building, Crowmarsh Gifford, Wallingford OX10 8AB, UK

stephen.king@stfc.ac.uk

hpj@ceh.ac.uk

Estimation of PHA Concentrations

The degree to which a mineral phase binds a humic substance depends on many variables (e.g. the mineral, the humic substance, the pH, ionic strength and dominant cation). The synthesis of all these factors is the adsorption isotherm, which relates the adsorbed amount Γ to the *equilibrium* PHA concentration C_e . But from an experimental perspective it is actually the *initial* PHA concentration C_i that determines how much PHA must be added to a sample. This may be calculated as

$$C_i = \frac{1000 \cdot \Gamma \cdot m}{V} + C_e \quad (\text{Equation SI-1})$$

for C in mg/l, Γ in mg/g, m (the mass of mineral) in g, and V (the volume of the sample) in ml.

Equation SI-1 can be taken a stage further if the isotherm data follows an established model. In the case of a Freundlich-type isotherm

$$\Gamma = K_F \cdot C_e^z \quad (\text{Equation SI-2})$$

where K_F is a measure of the strength of the adsorbate-adsorbent binding and the exponent z characterizes the heterogeneity of the distribution of binding sites (homogeneous if 1).

Substituting these expressions into one another then yields

$$C_i = \frac{1000 \cdot m \cdot K_F^x}{V} \cdot C_e^z + C_e \quad \text{or} \quad C_i = C_m \cdot K_F^x \cdot C_e^z + C_e \quad (\text{Equation SI-3})$$

if the concentration of mineral is C_m (in g/ml). The second exponent x (normally unity) can be used to refine the calculation to match a *known* value of C_i .

We have taken advantage of the work of Feng *et al* (1) who have measured the isotherms, and then extracted values of K_F and z , for the adsorption of a PHA onto montmorillonite and kaolinite at two

different ionic strengths of two different cations at two different pH's. Unfortunately none of their parameter space exactly matches our experimental system and consequently we have simply taken an average of their values across ionic strength (0.001 – 0.01 M) and pH (4 – 7) for adsorption onto montmorillonite in a Ca^{2+} electrolyte; for which we obtain $K_F = 1.7$ and $z = 0.4$. This yields the isotherm shown in Figure SI-1 below. Comparing it with the isotherms reported by Feng *et al* suggests that it represents adsorption which is neither overly strong nor overly weak. We then elected to use concentrations of PHA in our system that would deliver values of C_e of approximately 20 and 40 mg PHA/l, intended to correspond to 'low' and 'high' surface coverage scenarios, respectively (2).

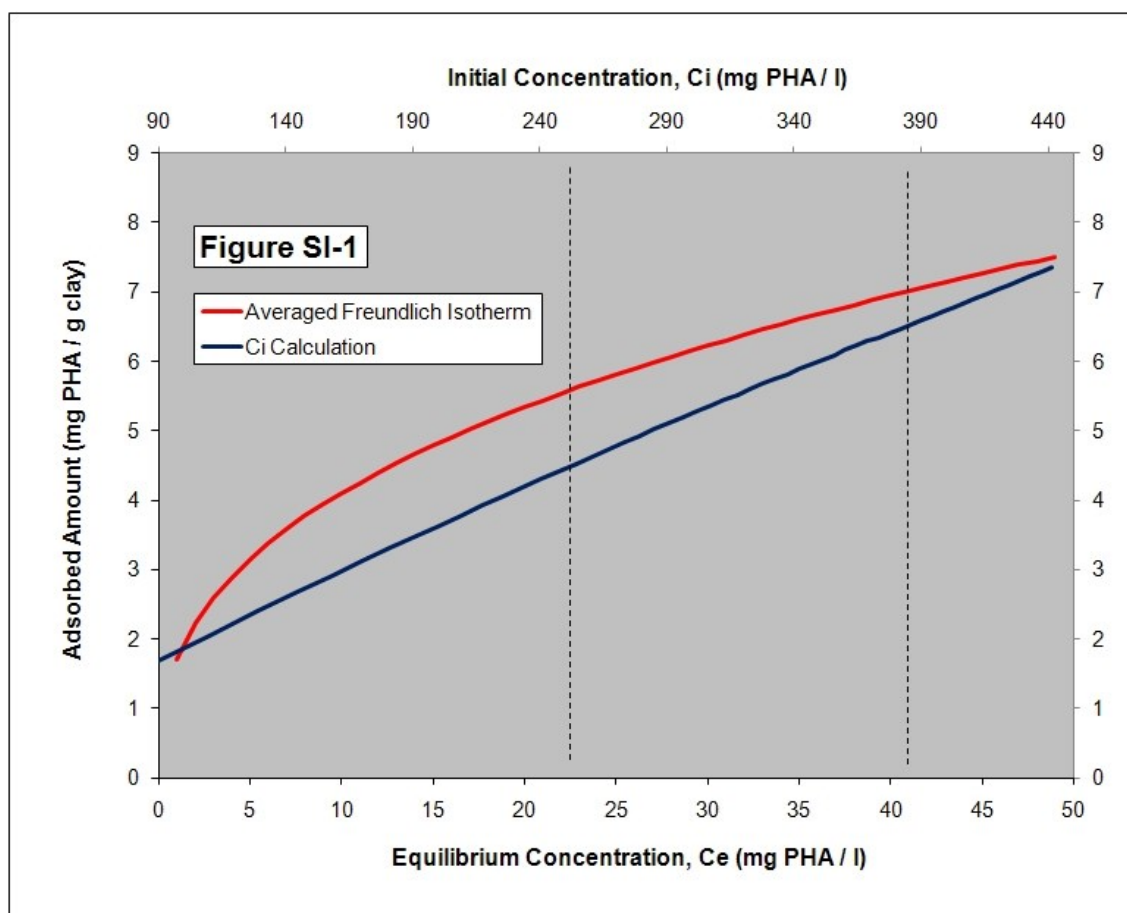


Figure SI-1. The adsorption isotherm used to estimate the amount of PHA to be added to the peroxide-treated sediment. The dashed vertical lines correspond to the 'low' and 'high' coverage scenarios investigated.

In our view it is a great pity that more adsorption studies in the literature do not report model fits to their isotherm data. Not only would this add important detail to those individual studies, it would also permit the wider exploitation of a valuable resource.

Percentage Composition of the Sediment and Empirical Formulae

The following data for the Priors Farm sediment is reproduced from Reference (3a).



SiO ₂	MgO	Al ₂ O ₃	Na ₂ O	Li ₂ O	CaO	F	P ₂ O ₅	K ₂ O	TiO ₂	MnO	Fe ₂ O ₃	FeO
60.5	0.81	13.16	0.15	<0.01	2.93	<0.01	0.76	2.14	0.86	0.14	5.89	<0.01

Representative SANS Data

Figures SI-2 and SI-3 depict fully corrected SANS data from selected samples. The scattered intensities $I(Q)$ have been normalized for the slight variations in volume fraction ϕ between samples as mentioned in the main text. The ‘E’ numbers are the experimental sample codes.

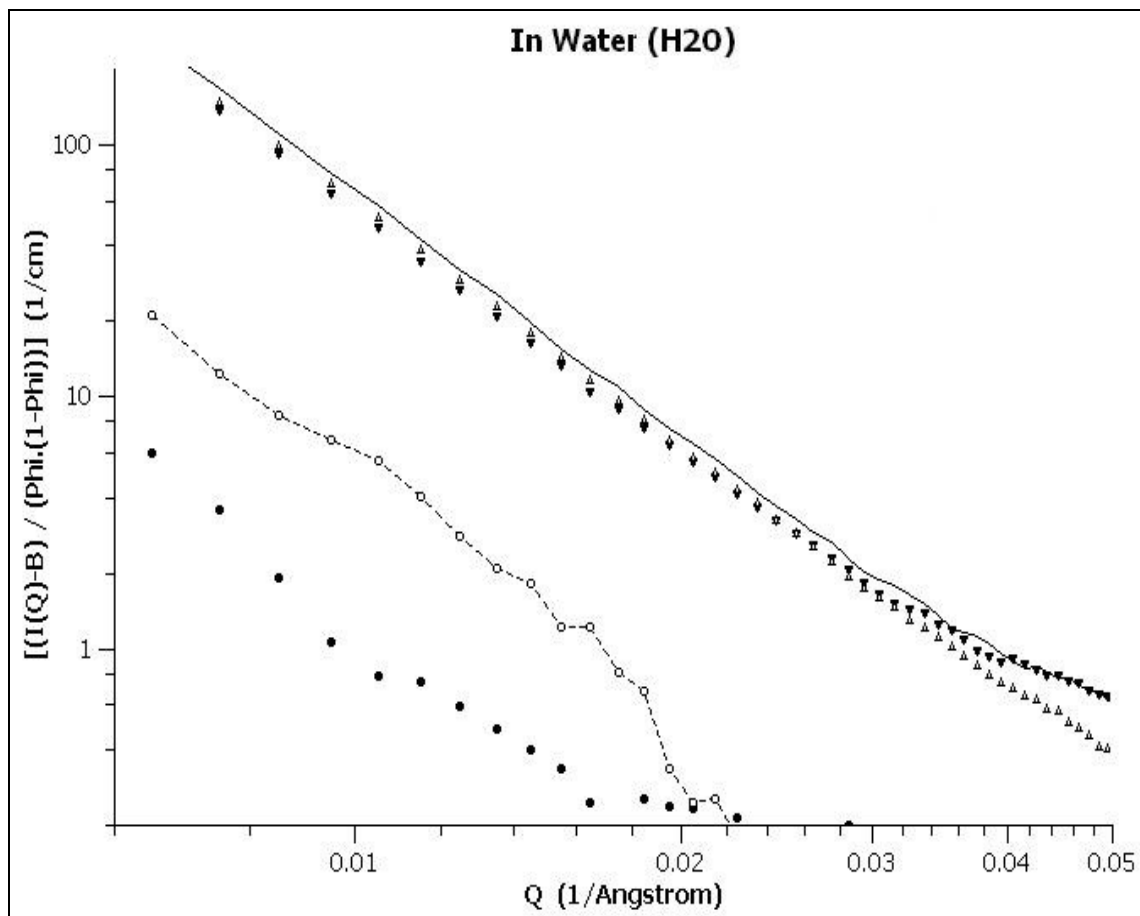


Figure SI-2. SANS from samples in deionised water: (—) untreated wet sediment, ‘E1.1’; (▼) *long-term* peroxide-treated sediment, ‘E1.11’; (△) peroxide-treated sediment + 380 mg PHA/l at pH6, ‘E3.2’; (-O-) the subtraction ‘E3.2’ *minus* ‘E1.11’; (●) 380 mg/l PHA solution, ‘B6’. Error bars are omitted for clarity. The approximately Q^{-3} fractal (power-law) scattering from the sediment samples is clear to see. The difference data, connected by the dashed line, indicate an enhancement of the scattering from the PHA in the presence of the mineral component, over and above that expected if it were simply solubilised. This suggests that PHA is adsorbed to the mineral surfaces.

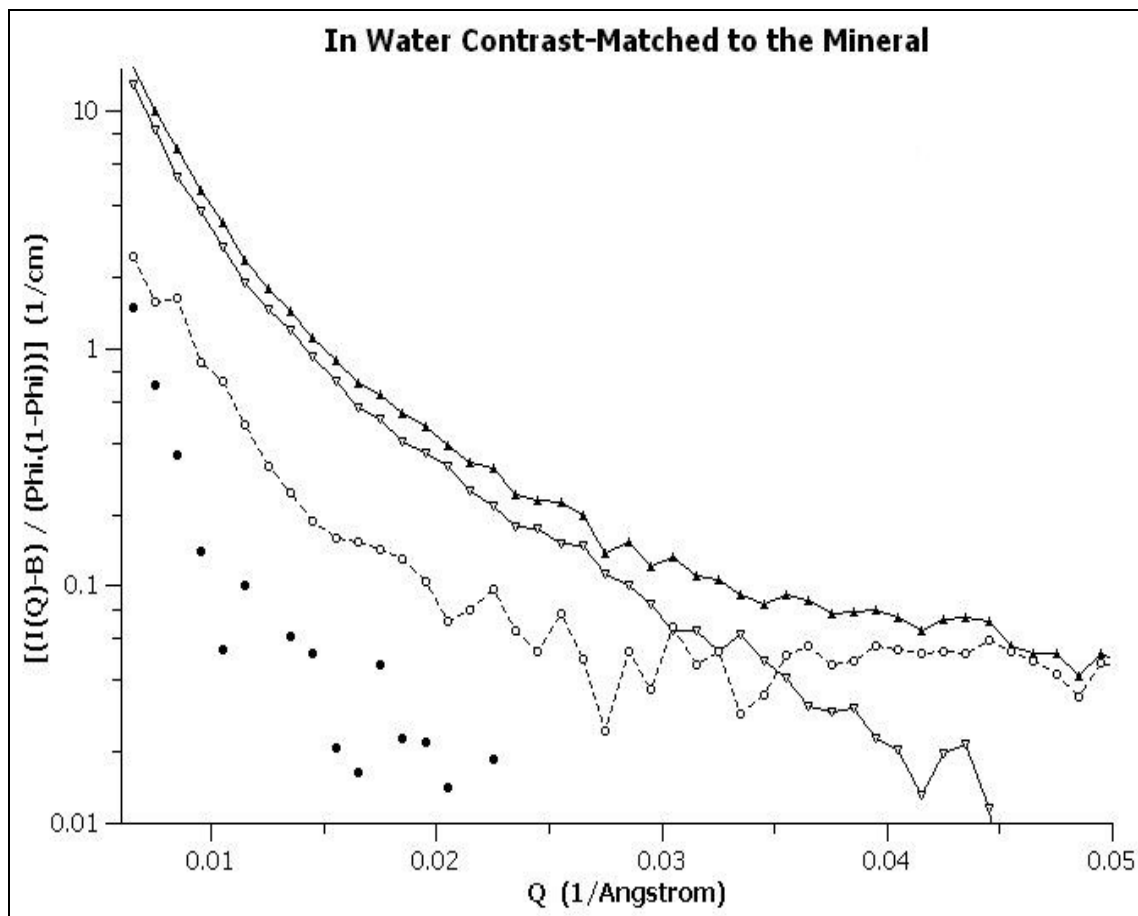


Figure SI-3. SANS from samples in a 34% : 66% H₂O : D₂O ‘contrast match’ mixture designed to suppress the scattering from the sediment mineral phase: (-▽-) peroxide-treated sediment, ‘E2.14’; (-▲-) peroxide-treated sediment + 380 mg PHA/l at pH6, ‘E3.8’; (-O--) the subtraction ‘E3.8’ minus ‘E2.14’; (●) 380 mg/l PHA solution, ‘B9’. Error bars are omitted for clarity. An order of magnitude reduction in scattered intensity for these samples, compared to Figure SI-2, is clear. Notice also that these contrast-matched sediment samples exhibit a different fractal power law. The difference data, connected by the dashed line, represent the scattering from the adsorbed PHA (plus a small contribution from any excess solubilised in solution).

Another SANS Scattering Law: The Polydisperse Fractal Cluster Model

In the Supporting Information to our earlier work (3b) we described at some length a variety of scattering ‘laws’ with the potential to provide information about the underlying nanostructure in natural aquatic nanocolloidal systems. Since that work another model has been brought to our attention and we have made extensive use of that model in the present study. The new model describes a system of polydisperse fractal clusters in turn composed of monodisperse spherical primary particles (4, 5, 6, 7) and may be expressed as

$$"I(Q)" = \frac{d\Sigma}{d\Omega}(Q) = (\rho_{cluster} - \rho_{medium})^2 \cdot \phi_{cluster} \cdot \phi_{medium} \cdot V_{primary} \cdot \frac{N_{agg}}{\Gamma(2 - \tau)} \times \quad (\text{Equation SI-4a})$$

$$\left[F(3 - \tau, Q\psi) (1 + Q^2\psi^2)^{-D_m(3-\tau)/2} + G(2 - \tau, Q\psi) \left(\frac{Q\psi}{h} \right)^{-D_m} \right] + B \quad (\text{Equation SI-4b})$$

where Q is the scattering vector, ρ is the neutron scattering length density, ϕ is the volume fraction ($\phi_{cluster} + \phi_{medium} = 1$), B is the background, D_m is the mass fractal dimension, N_{agg} is the average number of primary particles per cluster, τ is a polydispersity index (smaller is broader), $\Gamma(a)$ is the gamma function, $\Gamma(a,b)$ is the incomplete Euler gamma function, and

$$V_{primary} = (4/3) \cdot \pi \cdot R_{primary}^3; \quad (\text{volume of primary particle}) \quad (\text{Equation SI-5})$$

$$R_{g,primary}^2 = (3/5) \cdot R_{primary}^2; \quad (\text{radius-of-gyration of primary particle}) \quad (\text{Equation SI-6})$$

$$\psi = h \cdot R_{g,primary} \cdot N_{agg}^{(1/D_m)}; \quad (\text{correlation length}) \quad (\text{Equation SI-7})$$

$$h = \sqrt{\frac{D_m (D_m + 1)}{6}} \quad (\text{Equation SI-8})$$

$$u = \left[\frac{h^2 \cdot (1 + Q^2 \psi^2)}{Q^2 \psi^2} \right]^{D_m/2} \tag{Equation SI-9}$$

$$F(a, x) = \Gamma(a) - \Gamma(a, u) \tag{Equation SI-10}$$

$$G(a, x) = \sin \left[\frac{(D_m - 1) \cdot \pi}{2} \right] \cdot \frac{\Gamma \left(a, \left(\frac{x}{h} \right)^{D_m} \right)}{(D_m - 1)} \tag{Equation SI-11}$$

Equations SI-4 through SI-11 were fitted to the SANS data to extract values of N_{agg} , D_m , τ , $R_{primary}$, and ψ , see Figure SI-4, whilst $\rho_{cluster}$, ρ_{medium} , $\phi_{cluster}$ and ϕ_{medium} were fixed at their experimental values.

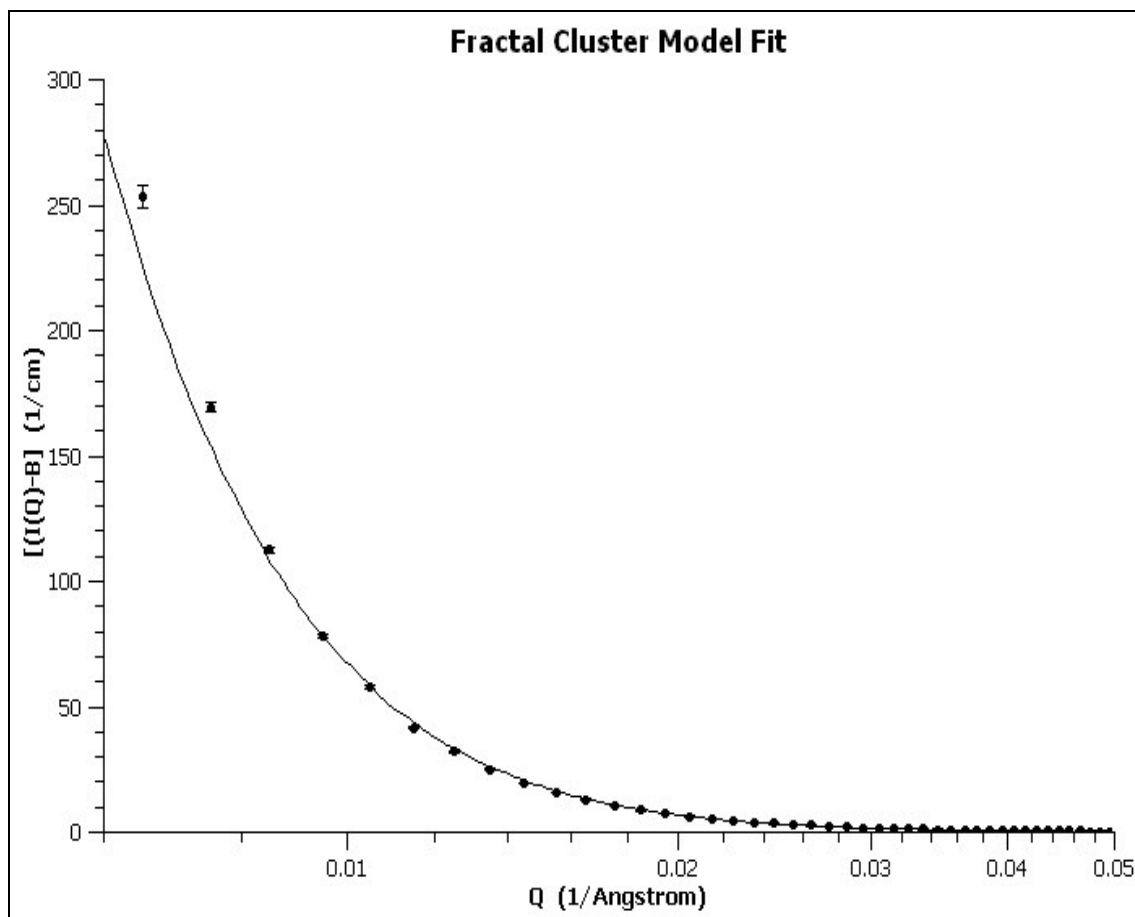


Figure SI-4. Example fit of the Fractal Cluster Model to the SANS data: (●) peroxide-treated sediment in 2 mM CaCl₂ + 255 mg PHA/l at pH6, ‘E3.3’; (—) model fit.

One caveat with the use of this model is that it assumes a single population of primary particles of a given composition. If more than one type of primary particle is present, and these are *simultaneously* highlighted by the contrast conditions, then Equation SI-4 will require, or return, some weighted-average particle size and composite polydispersity factor.

NB: In implementing this model we noted a long-standing typographical error that has been inadvertently propagated through the years. Equation 13 in (5), and Equation 7 in (7) (and, more recently, Equation 12 in Fratini *et al. Langmuir*. **2006**, 22, 306–312) all give the denominator in Equation SI-4a as $\Gamma(2-\pi)$ instead of $\Gamma(2-\tau)$ as used here, in Equation 15 in (5), and in (6).

SANS from Adsorbed Layers: The Surface Guinier Model

SANS has long been used by colloid and soft matter scientists to study the structure of adsorbed layers of surfactant or polymer on nanoparticle surfaces. A full explanation is beyond the scope of this Supporting Information but may be found in published literature (see for example 8, 9).

When the substrate particles are at contrast match with the dispersion medium, and in the absence of an interparticle structure factor $S(Q)$, the scattering from the adsorbed layer may be approximated as

$$"I(Q)" = \frac{d\Sigma}{d\Omega}(Q) = (\rho_{layer} - \rho_{medium})^2 \cdot \left[\frac{6\pi}{Q^2} \cdot \frac{\phi_{particle} \cdot \Gamma_{layer}^2}{\delta_{layer}^2 \cdot R_{particle}} \cdot \exp(-Q^2 \cdot \sigma_{layer}^2) \right] + B$$

(Equation SI-12)

where δ is the bulk density of the material in the layer, Γ_{layer} is the mass of material adsorbed per unit area (the adsorbed amount), and σ_{layer} is the second moment about the mean of the adsorbed layer thickness (the extent of the centre-of-mass of the layer). If the adsorbed layer were a neat, homogeneous, coating of constant thickness t , $\sigma_{layer} = (t^2 / 12)^{1/2}$.

Equation SI-12 was fitted to the SANS data to extract values of Γ_{layer} and σ_{layer} for different values of $R_{particle}$, whilst ρ_{layer} , ρ_{medium} , $\phi_{particle}$ and δ_{layer} were fixed at their experimental values. An example fit is shown in the main paper.

A valuable feature of Equation SI-12 is that it makes *no assumptions* about the actual surface distribution of the adsorbed material. However, as SANS tends to be relatively insensitive to very dilute concentrations of adsorbed material extending well away from the surface into the dispersion medium, this approach does underestimate the *maximum extent* of such adsorbed layers.

Contrast Factors

In SANS the ‘visibility’, known as the contrast, of the different components of a sample depends on the *square of the difference* in neutron scattering length densities ρ between a component and the dispersion medium (see Equations SI-4a & SI-12). The contrast factors relevant to this work are given in Table SI-1.

Table SI-1. SANS contrast factors, $(\rho_{component} - \rho_{dispersion})^2 (\times 10^{-20} \text{ cm}^{-2})$.

Dispersion	Mineral component	Organic component ^a
In 100% H ₂ O	20.7	3.8 – 7.6
In 34% H ₂ O : 66% D ₂ O	0.0	3.2 – 6.7
In 100% D ₂ O	5.5	17.2 – 24.5

^a This range of values is due to the uncertainty in the actual value of ρ . See (3a).

Literature Cited

1. Feng, X.; Simpson, A. J.; Simpson, M. J. Chemical and mineralogical controls on humic acid sorption to clay mineral surfaces. *Org. Geochem.* **2005**, *36*, 1553-1566.
2. Flerer, G. J.; Cohen Stuart, M. A.; Scheutjens, J. M. H. M.; Cosgrove, T.; Vincent, B. *Polymers at Interfaces*. Chapman & Hall. London. **1993**.
3. Jarvie, H. P.; King, S. M. Small-Angle Neutron Scattering Study of Natural Aquatic Nanocolloids. (a) *Environ. Sci. Tech.* **2007**, *41*, 2868-2873. (b) Supplementary Information for same.
4. Chen, S. H.; Teixeira, J. Structure and Fractal Dimension of Protein-Detergent Complexes. *Phys. Rev. Lett.* **1985**, *57*, 2583-2586.
5. Chen, S. H.; Rouch, J.; Tartaglia, P. Light Scattering from Polydispersed Fractal Clusters in Solution. *Croat. Chim. Acta.* **1992**, *2*, 353-366.
6. Rouch, J.; Tartaglia, P.; Chen, S. H. Experimental Evidence of Nonexponential Relaxation near the Critical Point of a Supramolecular Liquid Mixture. *Phys. Rev. Lett.* **1993**, *71*, 1947-1950.
7. Liu, Y. C.; Sheu, E. Y.; Chen, S. H.; Storm, D. A. Fractal structure of asphaltenes in toluene. *Fuel.* **1995**, *74*, 1352-1356.
8. King, S. M.; Griffiths, P. C.; Cosgrove, T. Using SANS to Study Adsorbed layers in Colloidal Dispersions. In *Applications of Neutron Scattering to Soft Condensed Matter*. Gabrys, B. J., Ed. Gordon & Breach. New York. 2000. Chapter 4.
9. King, S. M.; Griffiths, P. C.; Hone, J.; Cosgrove, T. SANS from Adsorbed Polymer Layers. *Macromol. Symp.* **2002**, *190*, 33-42.